PHILOSOPHICAL TRANSACTIONS OF THE ROYAL SOCIETY A MATHEMATICAL, PHYSICAL & ENGINEERING SCIENCES

Satellite Observations of Polar Ice Fields [and Discussion]

G. De Q. Robin, D. J. Drewry, V. A. Squire and A. S. Laughton

Phil. Trans. R. Soc. Lond. A 1983 **309**, 447-461
doi: 10.1098/rsta.1983.0054

Phil. Trans. R. Soc. Lond. A **309**, 447–461 (1983)
Printed in Great Britain

Satellite observations of polar ice fields

By G. de Q. Robin, D. J. Drewry and V. A. Squire
Scott Polar Research Institute, University of Cambridge, Lensfield Road, Cambridge CB2 1ER, U.K.

This paper outlines the research needed to advance the knowledge of polar ice masses that could be or has been provided by satellite techniques. Inland ice sheets, ice shelves and pack ice on polar oceans are discussed in separate sections. Because a satellite radar altimeter can cover wide areas of polar ice economically and rapidly, the interpretation of altimeter results is discussed in detail. Theoretical considerations are used to explain various characteristics of pulse shapes recorded over Antarctica by Seasat. Over inland ice, surface undulations cause the pulse shape to change rapidly with location, and the leading edge to migrate rapidly. Altimetry over ice shelves should be accurate to better than ± 1 m and provide new methods for studying their mass balance. Nearly all sea ice returns that have been studied show a characteristic glistening quite distinct from returns from the open ocean, inland ice or ice shelves. Reasons for glistening are presented and the need for ground truth stressed because pulse shapes should provide an additional source of data to define pack ice characteristics from satellite observations.

1. Introduction

Ice sheets in Greenland and Antarctica constitute 10 % of the surface land area of the Earth. Their accumulated 36×10^6 km^3 of ice comprises 90 % of global freshwater reserves. Sea ice covers a maximum global surface area of 24×10^6 km^2 during the northern summer, *ca.* 7 % of the world ocean surface. These ice masses are coupled closely with other aspects of the natural environment through complex exchanges of energy and mass (Radok 1978; Sergin 1979). An understanding of their dynamics and thermodynamics is fundamental to realistic global modelling of climatic, oceanographic and lithospheric processes. The investigation of ice masses, principally in polar areas, is hampered by extreme cold, long periods of darkness and persistent cloud cover in some areas. Remote sensing has and will play a critical role in the gathering of data and their routine surveillance.

This paper briefly reviews the most important research needs for the study of polar ice and points out where research can benefit from satellite techniques. Table 1 lists these needs for ice sheets and ice shelves and the contributions that have been made by satellite missions or those being planned. Table 1 of Gudmandsen (this symposium) lists similar requirements for the study of sea ice. These cover two types of data sets; one acquired within a time domain to study time-dependent changes such as sea-ice distribution and glacier dimensions, the other within a spatial domain where very detailed geographic coverage is required. Because of their importance to both types of study, techniques of radio altimetry from satellites are discussed in some detail.

2. Ice sheets

(*a*) *Surface form and ice dynamics*

It is not the continued existence of major ice sheets in remote polar regions that is of importance to mankind, but rather the possible global environmental effects of changes in these ice sheets on sea level, ocean circulation and climate. A first requirement in studying polar ice masses is

determination of significant changes. Landsat and other types of satellite imagery provide a rapid and accurate means of horizontal fixing and continued monitoring (to better than 100 m) of prominent surface features such as crevasse systems and the coastal boundaries of ice sheets. Imagery, whether at visual or infrared wavelengths or by radar methods, is not, however, satisfactory for mapping more critical parameters such as surface elevations or for providing data for glaciologists to assess ice sheet mass budgets.

Satellite altimetric methods, using radar altimetry with an accuracy of ± 1.0 m or better and laser altimetry with an accuracy of ± 0.1 m, have the potential to provide within one or two

TABLE 1. OBSERVATIONS REQUIRED FOR RESEARCH ON POLAR ICE SHEETS AND ICE SHELVES

glaciological parameter	required resolution	satellite measurement	satellites flown	satellites planned
surface morphology				
(i) large-scale	1.0 m	radar, laser altimetry	Geos-C Seasat	radar altimeter on ERS-1, TOPEX, Poseidon
		doppler	Transit–Tranet	—
		retro-reflector ranging		retro system on ERS-1
(ii) small-scale	0.5 m	laser altimetry, SAR	Seasat	SAR on ERS-1, Radarsat,
		MSS, TM, RBV	Landsat series	TOPEX, SPOT
ice thickness	5.0 m	—	—	future prospects limited
temperature field	1 K	inferred from microwave emissivity: ESMR, SMMR, LSR, VHRR, NEMS	Nimbus series, Tiros series, NOAA series;	radiometers (IMR) on ERS-1, MOS, Radarsat
accumulation or ablation				
(i) surface	0.1 m	(tentative relationship with microwave emissivity from ESMR)	Nimbus series NOAA series	ATSR/M on ERS-1 Radarsat
(ii) bottom	0.1 m	surface elevation changes of ice shelves	—	radar altimeter on ERS-1
velocity field				
(i) surface	0.5 m a^{-1}	doppler ranging	Transit/Tranet	retro system on ERS-1
		retro-reflector ranging	ARGUS	radar altimeter in ERS-1, TOPEX, SPOT, Poseidon
		altimeter backscatter matching: MSS, RBV	Landsat series	
(ii) internal or bottom	0.10 m a^{-1}			future prospects limited
dimensional fluctuations†	h = 0.1–0.5 m a^{-1}	h by radar + laser altimetry	Geos-C, Seasat	radar altimeter on ERS-1, SPOT, TOPEX, Poseidon
	L = 10 m a^{-1}	L by imaging MSS, TM, RBV, SAR	Landsat series, Seasat	SAR on Radarsat, TOPEX, SPOT, ERS-1
snowline position	10 m	microwave emissivities: ESMR, SMMR, VHRR	Nimbus, Tiros, NOAA, Landsat	ATSR/M on ERS-1, MOS, Radarsat

† h, surface elevation; L, margin position.

decades much more accurate and extensive information than present methods on changes in ice sheet volume. Once available, such information is simple to interpret and provides a straightforward answer to the present effect of ice sheets on the global hydrological cycle.

Simple monitoring of ice sheets by satellites will not, however, advance knowledge of ice dynamics to the point where it is possible to forecast future changes in ice sheets that result from climatic changes. For this we need a better understanding of ice sheet dynamics.

Full description of ice sheet dynamics requires knowledge of the seven parameters listed in

table 1, and a starting point is the relation between driving stress (τ), ice thickness (h) and surface slope (α):

$$\tau = \rho_i g h \sin\alpha, \tag{1}$$

where ρ_i is ice density and g is gravitational acceleration. Equation (1) is only effective when mean values of parameters over distances at least an order of magnitude greater than the ice thickness are used. Over short distances stress variations caused by ice flow over bedrock irregularities affects surface relief considerably. Satellite altimetry can determine values of α with greater accuracy, at much greater speed and at lower cost per unit area than by any other method (Robin 1966; Brooks *et al.* 1978). The other major variable, ice thickness, has been routinely measured for two decades by airborne radio echo-sounding techniques (Robin *et al.* 1969; Drewry 1981). The possibility of measuring ice thickness from satellites is not promising.

An early study by Nye (1951) treated ice as a plastic material with a constant yield stress (τ_0). Then for an ice sheet on a roughly horizontal bedrock with low surface slope $\alpha = \mathrm{d}h/\mathrm{d}x$ (x-flow direction), integration of (1) gave

$$h = \{2\tau_0 (L-x)/\rho_i g\}^{\frac{1}{2}}, \tag{2}$$

where L is ice-sheet half width. By 1958 this model did not fit new information on the form of the Greenland and Antarctic ice sheets. On the assumption that outflow was due to internal deformation in the absence of basal sliding, Vialov (1958) derived an improved expression for the surface profile of an ice sheet as

$$(h/H)^{2+2/n} + (x/L)^{1+1/n} = 1, \tag{3}$$

where H is thickness at the ice sheet centre and n is the viscoplastic parameter in ice flow law of Glen (1955), so with $n = 3$ we get

$$(h/H)^{2.7} + (x/L)^{1.3} = 1. \tag{4}$$

Weertman's (1957) equation for basal sliding velocity (U_b) in terms of basal shear stress τ_b, and a roughness parameter R is

$$U_b = C\tau_b^{\frac{1}{2}(n+1)}/R^{n+1}, \tag{5}$$

gave

$$(h/H)^{2.5} + x/L^{1.5} = 1. \tag{6}$$

According to Paterson (1981) both equations give a satisfactory fit to an observed profile for 800 km inland of Mirny on the Antarctic ice sheet.

Because $n \approx 3$, Weertman's theory suggests that the velocity due to sliding increases with the square of τ_b, whereas the surface velocity due to internal deformation (U_d) used to derive (3) from the vertical shear rate $\dot{\epsilon}_{xz}$ is given by

$$U_d = \int_0^z h\dot{\epsilon}_{xz}\,\mathrm{d}z \tag{7}$$

gives

$$U_d/h \propto \tau_b^3.$$

Logarithmic plots of τ against U_d/h for ice sheets in Budd & Jenssen (1975), Budd & Smith (1981) and Cooper *et al.* (1982) show a quasi straight-line relation with n ranging from 2.5 to 4, whereas corresponding plots of sliding velocity against τ_b show much greater scatter than would be expected if (5) applied.

It therefore appears that internal deformation explains the motion of interior regions of ice sheets reasonably satisfactorily, but it is clear that in outer regions sliding is the dominant mechanism in fast-flowing glaciers and ice streams that discharge a large proportion of the ice.

Surface undulations, over distances of a few times the ice thickness, superimposed on the mean slope (equation (3)) have been explained in terms of varying longitudinal and shear stresses in the ice mass (Robin 1967; Collins 1968; Budd 1970). Theory is now at the point where detailed surface profiling from satellites may make useful estimates of ice velocities possible.

(*b*) *Velocity field*

Surface velocities have been successfully measured by satellite systems by using Transit–Tranet doppler ranging. While the accuracy of this method is limited to 1 or 2 m., and is thus not suitable for short-term monitoring of slow-moving interior regions of Antarctica and Greenland, it has proved adequate for ice shelves where velocities greater than 0.1 km a^{-1} are usual (Thomas 1979). The technique is restricted in that a ground station has to be deployed on the ice on at least two occasions, and occupied for a minimum of 2–3 days for maximum accuracy. Further needs are information on the variation of velocity with depth, and basal sliding velocities. Both are as yet unobtainable by satellite.

(*c*) *Temperature field*

The surface and internal temperature of ice sheets play important roles in ice dynamics. Ice creep rate is temperature-controlled. Whether or not basal sliding takes place is largely determined by the balance between geothermal and frictional heat and cold carried down from the upper surface by ice motion.

Approximate temperatures in the upper few metres of ice sheets may be estimated, given adequate calibration, by passive microwave radiometry. Measurements may be made at single or multiple frequencies. An initial application of satellite radiometry to ice used the ESMR (150 mm wavelength) on Nimbus-5 (Zwally & Gloersen 1977). A major problem in interpretation is the correlation of physical temperature with emissivities, which are also affected by crystal size or grain size due to scattering and absorption.

(*d*) *Accumulation rate*

This is a basic input parameter to all studies of ice-sheet modelling. No effective airborne or satellite methods of measuring accumulation rates are known, although there does appear to be a link between microwave emissivities mentioned above and accumulation rates through a relation with crystal size and fabric of surface layers of cold ice sheets. Such information is largely qualitative in suggesting areas of very low accumulation rates in central Antarctica (Zwally & Gloersen 1977).

(*e*) *Dimensional changes*

Satellite radar altimetry with an accuracy of ± 1.0 m is adequate to map within several years the major changes in vertical height of ice sheets that may be associated with surging of a basin on an ice sheet, or slower changes of the order of 1.0 m a^{-1} over a decade, (suggested by Mae & Naruse (1978)). In central Antarctica changes of 0.01 m a^{-1}, which represent a significant imbalance of around 35 % total accumulation, require a relative accuracy of elevation measurement of around 0.1 m a^{-1} over two decades for detection. Surface elevation changes at Camp Century in Greenland and Byrd Station, Antarctica, for example, may be $+0.03$ m a^{-1} and -0.03 m a^{-1} respectively (Budd *et al.* 1971) and should be detected by laser altimetry to ± 0.1 m over one decade.

PHILOSOPHICAL TRANSACTIONS OF THE ROYAL SOCIETY A MATHEMATICAL, PHYSICAL & ENGINEERING SCIENCES

3. Ice shelves

Floating ice shelves exist around *ca.* 55 % of the periphery of the inland ice sheet of Antarctica (Drewry *et al.* 1982). Ice shelves are formed principally from inland ice discharged into the sea, and by the accumulation of snow on fast ice. The flow of ice shelves takes place by spreading and forward motion over a virtually frictionless base. The driving stress governing spreading is proportional to the weight of ice above sea level, $\bar{\rho}_i g E$, where E is surface elevation and $\bar{\rho}_i$ is mean ice density above sea level, or equally by the buoyancy upthrust on ice below sea level, $|(\rho_w - \rho_i)\, g h_w|$, where ρ_i and ρ_w are the mean densities of ice and sea water and h_w is the ice draught below sea level. Ice thickness $h_i = E + h_w$, and for hydrostatic balance

$$\int_0^{h_i} \rho_i\, g h \,\mathrm{d}h = \rho_w g h_w. \tag{8}$$

The driving stresses produce horizontal strain rates $(\dot{\epsilon}_x, \dot{\epsilon}_y)$ that may be partly balanced by accumulation rates on top and bottom surfaces – the latter by ice frozen from the sea, and by the flow of ice from inland. Ablation on Antarctic ice shelves is mainly bottom melting and also affects strain rates. Drag at side boundaries and due to local grounding has to be considered. Normally ice shelves thicken inland from the ice front.

Bottom melting and freezing takes place beneath ice shelves, but relevant observations are few and mainly apply near the ice front, where melting is expected to be high (Thomas 1973; Crary 1962; Swithinbank 1962; Zotikov *et al.* 1980; Jacobs *et al.* 1979). Indirect estimates of the presence or absence of bottom melting based on the nature of radio echo reflexions from the ice–water interface (Neal 1979; Robin *et al.* 1983) indicate wide variations in bottom melting–freezing with location.

We expect (8) to apply over most of the ice shelf, exceptions being areas close to ice shelf boundaries, to local grounding, and where extensive shear between ice streams of different velocities and thickness occurs. Even though satellites may not measure ice thickness directly, accurate measurements of surface elevation by satellite altimetry and use of (8) should make it possible to map ice shelf thickness. This should be based on comparison of extensive radio echo values of thickness (h_i) of Antarctic ice shelves with surface elevations from satellite altimetry, because the variation of ρ_i, ρ_w and g with location is small. Measurement of ice shelf surface elevations from satellites to an accuracy of ± 1.0 m should then make it possible to determine ice thickness accurate to ± 10 m, a useful accuracy for ice shelf dynamic studies. Increasing the accuracy to ± 0.1 m in elevation, as may be possible over level ice shelves, may give ice thicknesses accurate to ± 1.0 m, an accuracy sufficient to determine significant changes of ice thickness from bottom melting at a specific geographical point in a few years, but this demands more rigorous knowledge of $\bar{\rho}_i$ and ρ_w. Satellite altimetry should thus open up a new method of studying the mass balance of ice shelves. A further example may be given. Unlike inland ice, where surface undulations caused by ice flowing over bedrock irregularities appear to be fixed in space, surface rolls and chasms on ice shelves are carried forward by the motion of the ice. Accurate fixing of these features by satellite imagery should enable measurement of ice velocity from satellites to be made.

The study of the calving of icebergs should benefit from repeated collection of MSS-type imagery over a number of years, and provide enough basic data for the development of adequate theory. Already lower-resolution imagery from Nimbus and other satellites has provided information on

PHILOSOPHICAL TRANSACTIONS OF THE ROYAL SOCIETY A MATHEMATICAL, PHYSICAL & ENGINEERING SCIENCES

the calving of some major icebergs and produced evidence that collision of large icebergs with glacier tongues and ice shelves can be a relatively frequent cause of fracture and formation of icebergs (Swithinbank *et al.* 1977). Tracking of large icebergs on these images also shows the major oceanic circulation. More extensive information has been obtained by tracking transponders on smaller Antarctic icebergs (Tchernia 1974).

4. Sea ice

Sea ice is spatially and temporally one of the most variable natural materials found on the Earth's surface. Its character and morphology depend critically on its age, and on climatic and oceanographic factors prevalent during its growth and subsequent lifetime. Its growth is well documented in the polar literature. First, minute spherical ice crystals form at the sea surface, which quickly evolve into thin discoids of 1–3 mm diameter and 1–10 μm thickness. These rapidly spread laterally to form a suspension, which gives the sea a soupy appearance, called *frazil* ice. Unless oceanic conditions are remarkably calm, ocean waves and currents break up the frazil to form either *pancake* ice or a thick polycrystalline slurry of frazil platelets in concentrations between 20 and 40 % known as *grease* ice (Martin 1981). Once formed, sea ice growth proceeds rapidly under the control of prevailing atmospheric and oceanic conditions.

Young ice (less than 0.3 m thick) and first-year ice (0.3–2 m) are more saline than older sea ice and are often made up of three layers of different crystallographic structure. Beneath the snow cover but near to the upper surface, the ice is polycrystalline, with typical salinities between 5 and 15 ‰. Under this layer lies a region of vertical columnar crystal growth with significantly lower salinity (4–5 ‰). During growth the ice in contact with the underlying sea water forms a thin layer, of high salinity (30 ‰) and low mechanical strength, known as the skeletal layer.

Second-year and multiyear ice are very different from younger sea ice. Pressure ridges with sails up to 10 m high and keels down to 40 m depth can be formed during its growth, due to compressional and tensile stresses in the ice cover brought about by changes in ocean currents and winds. The summer melt cycle also serves to alter the properties of Arctic sea ice by metamorphosis of the ice surface into an array of refrozen meltponds and hummocks. Beneath this, the columnar structure and skeletal layer are preserved, but salinities are substantially less (due to desalination within the bulk of the ice) and crystal sizes substantially larger. This broad classificatory scheme for sea ice overlooks several important factors that can change its basic properties. Rate of growth, for example, will determine salinity and also crystal fabric. Furthermore, grease ice crystals can sinter to form irregular clumps of ice, which grow very rapidly to produce a sea ice of different character that may be much more widespread in Antarctic sea ice than in the Arctic. The presence of a significant snow cover during growth can also change the composition of sea ice by insulating its upper surface or by depressing the ice sufficiently to cause infiltration by brine. Again this is probably more frequent in Antarctic waters than in the Arctic Ocean. In altering the character of sea ice these effects are significant for the interpretation of satellite remote-sensing imagery.

Gudmandsen's table 1 (this symposium) lists a set of key glaciological needs for the study of sea ice and its relations with climate and the oceans. In this context, the main role of sea ice is to inhibit the exchange of heat, moisture and momentum between atmosphere and ocean.

The location of the ice edge and the morphology and distribution of ice floes within the Marginal Ice Zone (MIZ) are important and little-understood parameters in both climatological and

PHILOSOPHICAL TRANSACTIONS OF THE ROYAL SOCIETY A MATHEMATICAL, PHYSICAL & ENGINEERING SCIENCES

oceanographic modelling studies. Within the MIZ the distribution of floe sizes will be determined by, *and will determine*, the ocean wave energy found at any location. Waves penetrating the pack from the open sea will fracture ice floes if the floes are too large to exist in waves of that height (Robin 1968; Goodman *et al.* 1980). Waves are also attenuated by the pack, with the energy decaying as a function of wave period and ice characteristics encountered en route (Robin 1963; Wadhams 1975, 1978; Squire & Moore 1980). Thus the ultimate floe size at any position within the MIZ is under the control of waves from the open sea and of the local oceanographic and meteorological effects that redistribute the ice cover. Once determined, floe size distribution is crucial to a thorough understanding of MIZ oceanic processes.

The concentration of ice floes in any ice-covered region represents a delicate balance of wind, waves and ocean currents that will be upset by meteorological or oceanic disturbances. We therefore see concentration as a sensitive marker of change and as an indicator of zones of divergence or compressive motions within the pack ice.

The concept of an individual ice floe is difficult to apply to the central Arctic Ocean where hundreds of square kilometres are totally ice-covered with little evidence of open water except for occasional sinuous leads or polynyas. Pressure ridges form the only relief and determine surface roughness characteristics in a particular region. A detailed knowledge of their distribution is essential if measured values of form drag coefficients for different ice surfaces are to be incorporated into the momentum balance equations so that realistic and reliable global weather predictor models may be routinely implemented.

No remote sensing method has yet been able to measure thickness accurately for all types of sea ice. Initial successes with impulse radar-type measurements are limited to ice of low salinity, and new ice of any reasonable thickness has evaded measurement. Satellite imagery at certain wavelengths, passive microwave emission data, scatterometry, altimeter pulse shapes and synthetic aperature radar all combine to provide information that helps to identify the ice type and concentration present in any region. From this a qualitative estimate of ice thickness may be made and estimates made of the heat exchange between the ocean and atmosphere.

5. Satellite altimetry

Mapping the Antarctic ice sheet by satellite radar altimeter was proposed by Robin (1966), whereas Zwally (1975) suggested that the technique could be used to determine changes in elevation of ice sheets. Results from Geos-C showed a repeatability better than 3 m over Greenland (Brooks *et al* 1978), and better than ± 1 m from Seasat data over Antarctica (Brooks 1982). The figure for repeatability is relevant to determination of changes of surface elevation, but for mapping, satellite altimetric data should be corrected for deformation of the geoid.

The altimeters on Geos-C and Seasat were designed for the study of ocean surfaces. Systems developed for tracking echoes have not proved entirely satisfactory over ice sheets, where the lock frequently failed. Wide variations in the returned echo pulse shape and strength found with Geos-C and Seasat data also provide useful information about the nature of the reflecting surface, so we discuss the factors controlling pulse shape at some length.

The main characteristics of satellite radio altimeters and of an airborne system used to sound polar ice thickness are shown in table 2. While the airborne system uses a lower frequency and longer pulse length than the satellite altimeters, the geometry of the echo from the base of the ice has many features that are relevant to the interpretation of satellite radar altimetry.

PHILOSOPHICAL TRANSACTIONS OF THE ROYAL SOCIETY A MATHEMATICAL, PHYSICAL & ENGINEERING SCIENCES

We consider a pulse of square form with a pulse width of 3 ns transmitted from a satellite at 800 km height. This spreads as a spherical wave within limits governed by the antenna beamwidth. When the end of the pulse reaches a flat surface, the pulse will cover a circular area of diameter around 1.6 km. Thereafter the pulse will spread out as an annulus around the nadir point until limited by the antenna beamwidth to a diameter *ca.* 22 km for Seasat. The pulses shown later, in figure 1, are limited by the time gate to a diameter around 9 km on a flat surface.

Three types of reflecting surface discussed in Robin *et al.* (1969) should be considered.

TABLE 2. RADAR ALTIMETER CHARACTERISTICS

	Skylab	Geos-C (intensive mode)	Seasat	ERS-1	N.S.F.–S.P.R.I.–T.U.D. radio-echo sounder†	
mean altitude/km	435	843	800	777	0.3	operating height above terrain/km
antenna beamwidth/deg	1.5	2.6	1.6	1.2	20 × 120	antenna beamwidth/deg (sideways, fore-aft)
frequency/GHz	13.9	13.9	13.5	13.7	0.06 and 0.3	frequency/GHz
peak power/kW	2	2	2	0.5	1–10	peak power/kW
pulse width/ns (uncompressed)	130	1000	3200	*ca.* 5000	60–1000	pulse width/ns (uncompressed)
pulse width/ns (compressed)	10	12.5	3.1	3	63	pulse width/ns (compressed)
pulse repetition frequency/Hz	250	100	1020	*ca.* 1000	12.5–25	pulse repetition frequency/kHz
pulse-limited footprint diameter/km	8	3.6	1.6	1.6	0.05 × 0.5	beam-limited footprint/km (at surface)
altimeter precision/m (r.m.s.)	< 1	< 0.05	< 0.01	0.01	1.25	altimeter precision/m (r.m.s.).
orbit/deg	50	± 65	± 72	± 82	—	—

† National Science Foundation – Scott Polar Research Institute – Technical University of Denmark.

1. *Plane polished reflector.* In this case any departure from a plane surface is small compared with the radio wavelength (λ). If P_t is the transmitted power, g_t the antenna power gain along its axis, S_r the effective absorption cross section of the receiving antennae, r_0 the range to the reflecting surface and R_n the power reflexion coefficient of the reflecting surface at normal incidence, the received power P_r is given by

$$P_r/P_t = R_n g_t S_r/16\pi r_0^2. \tag{9}$$

2. *Perfect diffuse reflector.* This reflects a fraction (R_d) of incident radiation into a hemisphere according to Lambert's law. The flux per unit angle reflected in a direction ϕ to the normal to the surface is proportional to $\cos\phi$ so that, in optical terms, the surface has equal brightness from all viewing directions. For near-normal angles, a plane reflecting surface, and with certain qualifications concerning polarization, we have within the pulse-limited footprint

$$P_r/P_t = R_d g_t S_r v t/4\pi r_0^3, \tag{10}$$

where v is the radio wave velocity and t is the time after arrival of the leading edge of the pulse. P_r rises linearly until time t_p, the pulse length, after which the reflecting annulus is of approximately constant area so that P_r is approximately constant within the beam-limited footprint.

3. *Extended rough surfaces.* We consider a surface in which slopes are uniformly distributed up to some maximum value (β_{max}), which is not large. Backscattering in the direction of incidence

has been analysed by Beckmann & Spizzichino (1963), who consider that this scarcely varies at normal incidence between models of varying complexity. We consider two cases.

(i) When the surface consists of random irregularities of all sizes down to $\lambda/2\pi$ or less in the horizontal plane, Booker *et al.* (1950) showed that the surface behaves like a Lambert-law reflector.

(ii) When individual facets of the surface are flat to a small fraction of a wavelength over dimensions large compared with the wavelength, the problem becomes one of geometrical reflexion as with the optics of a 'glistening surface' defined by $\phi_p < \phi < \beta_{max}$, where ϕ_p is the angle of the pulse-limited footprint. We assume that the power reflected by individual facets is in a random phase relation to its neighbours and the average power received is the sum of the individual powers. For a square pulse, the echo rises to an initial maximum given by

$$P_r/P_t = \frac{R\lambda^2 g_t^2}{64\pi^2 r_0^{2.5}} \frac{(vt_p)^{\frac{1}{2}}}{\beta_{max}}, \tag{11}$$

after which the power falls approximately in proportion to $t^{\frac{1}{2}}$ until a time t_β when it will fall abruptly to zero; t_β is related to β_{max} by

$$\beta_{max} = (2vt_\beta/r_0)^{\frac{1}{2}}. \tag{12}$$

When $\beta_{max} = \phi_p$, $t_\beta = t_p$, and since $Sr = g_t\lambda^2/4\pi$ we have, from (11) and (12),

$$P_r/P_t = \frac{Rg_t S_r}{16\pi r_0^2} \frac{1}{\sqrt{2}}, \tag{13}$$

which differs from (9), for example, by only $\sqrt{\frac{1}{2}}$, or around 1 dB. Thus for $\beta_{max} < \phi_p$ in this case it appears reasonable to treat the maximum returned power as equal to that given by specular reflexion.

Fading range and fading rate. Owing to satellite motion, phase changes between reflecting facets that are not resolved in range cause a calculated fading rate on Seasat records up to around one cycle per metre of path length compared with a spacing along track of *ca.* 6.6 m between pulses. This suggests a random distribution of returned energy with a Rayleigh distribution, in which case the fading range will be 13.4 dB, which is of the order of the Seasat observations over the oceans. To reduce this scatter the returned energy in each gate was averaged over 50 pulses and two 50 pulse averages were combined for data transmission. This gave statistical smoothing by a factor of 10. This was effective over the oceans, but over 600 m of an undulating ice sheet systematic drift in energy returns may be of magnitude comparable with statistical fluctuations.

6. Seasat pulse data

(*a*) *Introduction*

Some typical Seasat pulse shapes obtained during a single crossing of Antarctica in 1978 are shown in figure 1. The horizontal scale of time is linear and divided into 60 intervals, for each of which the mean power is plotted on a linear scale. However, the plot has been normalized to fill the vertical scale, and figures on the left-hand scale indicate how much this scale has been expanded between successive plots.

Within each group (*a*) to (*e*) the recorded pulses are shown at one second (6.6 km) intervals, although data are available at one tenth of that spacing. The pulse shapes of groups (*a*) open

ocean, (*b*) ice shelf and (*c*) inland ice approximately fit our description for diffuse (Lambert's law) reflectors, whereas returns typical of a glistening surface are seen in groups (*d*) and (*e*).

(*b*) *Open ocean*

In figure 1*a* the open ocean surface is best described as an extended rough surface with random irregularities down to $\lambda/2\pi$ (3 mm) that produce reflexions that follow Lambert's law. The initial pulse rise time is governed by longer wavelengths as discussed by Cartwright and Tucker (both this symposium).

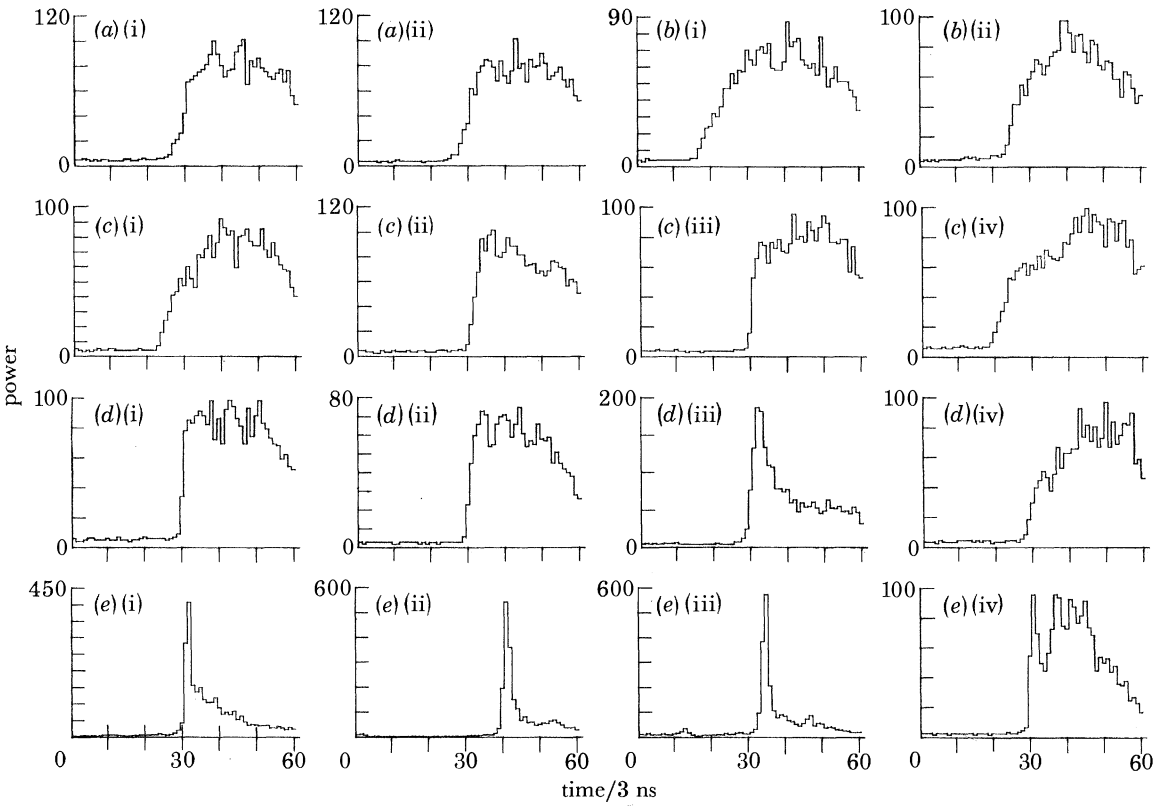

FIGURE 1. Altimeter pulse shapes recorded by Seasat during one crossing of Antarctica, showing power (linear scale) against time (60 intervals of *ca.* 3 ns). (*a*) Open ocean, 55.245° S, 56.794° E (i) to 55.196° S, 56.739° E (ii); (*b*) ice shelf, 67.537° S, 81.671° E (i) to 67.502° S, 81.544° E (ii); (*c*) ice sheet, 69. 363° S, 89. 539° E (i) to 69.277° S, 89.196° E (iv); (*d*) pack-ice–Ocean, 61.977° S, 67.036° E (i) to 61. 845° S, 66.781° E (iv); (*e*) pack ice, 66.165° S, 77.105° E (i) to 60.052° S, 76.768° E (iv).

(*c*) *Ice shelves*

In figure 1*b* only two pulse shapes are shown as the orbit just crossed a corner of the West Ice Shelf. The similarity of pulse shape to those of the open sea in figure 1*a* is even more apparent from longer series available on other orbits. The diffuse-type pulses are attributed to sastrugi on a near-horizontal and flat surface. There is no evidence of the 'glistening' effect found on sea ice. Over vast areas of ice shelves, the surface irregularities are small, so the resultant radio altimetric errors could be as small as those over the ocean, i.e. around 0.1 m. The use of such accurate ice shelf altimetry, discussed in § 3, should open up new approaches to research on ice shelves.

(*d*) *Ice sheets*

The pulse shapes obtained over the Antarctic ice sheet shown in figure 1*c* again indicate a diffuse reflector. There is, however, a greater variability of pulse shape over the ice sheet than in figure 1*a*, *b*. The rate of rise of the pulse and the position of the strongest return vary considerably and often the pulse ramp migrates rapidly across the time gate with a resultant inability to maintain tracking. These effects all result from large-scale undulations of the surface of the ice sheet.

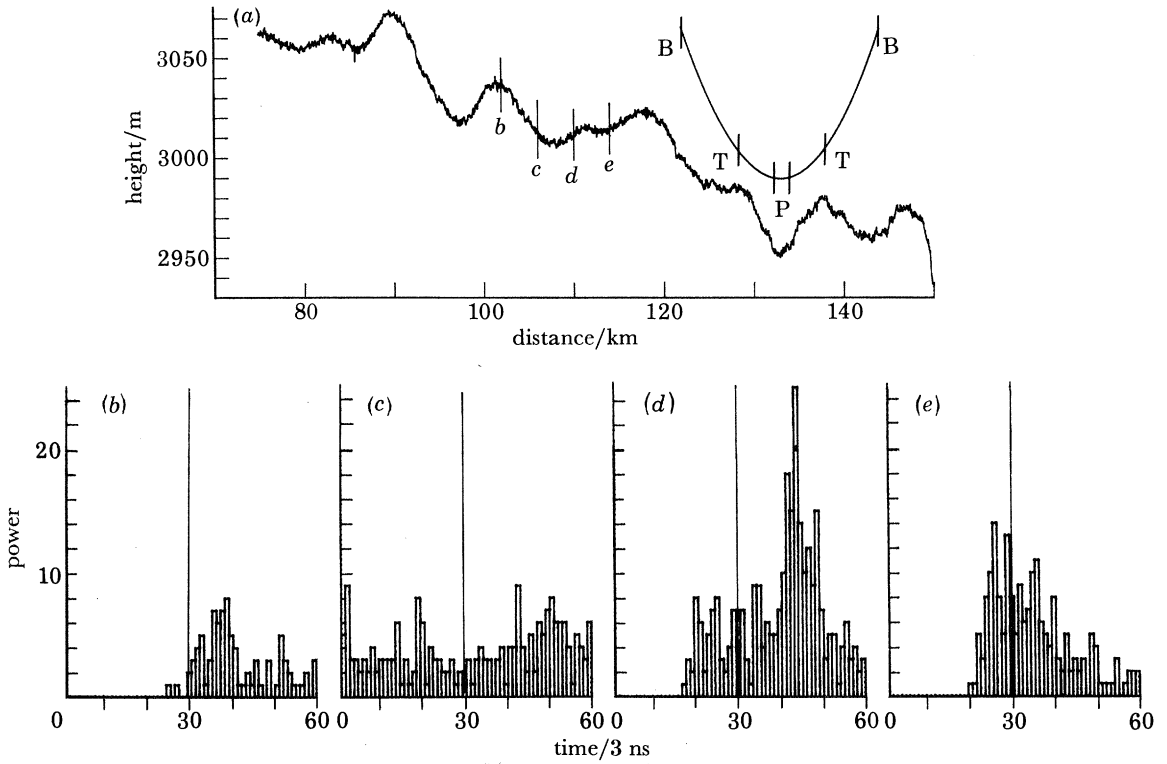

FIGURE 2. (*a*) Surface profile over the East Antarctic Ice Sheet from 88.96° S, 17.50° W to 88.32° S, 28.52° W from an aircraft radio altimeter record corrected by the aircraft pressure altimeter record by N. McIntyre. The shape of the altimeter pulse front from Seasat is shown in the upper right section, allowing for vertical scale exaggeration. Footprint widths over horizontal surfaces are shown for the beam-limited case (BB), for the time-gate limits used in figure 1 (TT) and for the pulse-limited footprint (P). The pulse length is about the same as the line thickness.

(*b*–*e*) Radio altimeter pulse shapes computed by M. R. Gorman for a two-dimensional model by using the profile in (*a*) and other characteristics as for Seasat and ERS-1. Resultant pulse shapes shown are those for corresponding nadir points (*b*) to (*e*) along the profile (*a*).

In figure 2*a* we show a typically undulating surface profile of the East Antarctic Ice Sheet near the South Pole from radar altimeter and pressure altimeter records of the N.S.F.–S.P.R.I.–T.U.D. flights. Also shown is the satellite altimeter pulse shape for a satellite height of 800 km. The pulse length (Seasat and ERS-1) of 1 m is similar to the line width. We see that large-scale curvature of the ice surface is comparable with and at times is greater than that of the altimeter pulse, so that over a valley the first return to the satellite will come from the valley sides rather than the bottom of the valley.

PHILOSOPHICAL TRANSACTIONS OF THE ROYAL SOCIETY A MATHEMATICAL, PHYSICAL & ENGINEERING SCIENCES

A two-dimensional computer analysis of the pulse shapes that would be returned to a satellite (Seasat or ERS-1) by the surface is shown in figure 2*b–e*. For a flat surface the two-dimensional model returns a pulse that will fall in proportion to $\sqrt{t}$ instead of remaining approximately constant as in the three-dimensional model. Nevertheless, the analysis shows similar effects of surface undulations to those shown in figure 1*c*. The analysis was centred on the nadir point from the satellite, so the pulse migrates as surface slopes change.

In figure 2*b* the nadir point on a convex upward surface produces a weak return that falls rapidly with time. Figure 2*c*, over a sloping surface, causes the first return to migrate off the time window. This could cause a tracking failure. Figure 2*d* shows an initial rise somewhat stronger than in figure 2*b* followed by a substantial rise due to the combined effects of concave upward surfaces at 110 and 114 km. Figure 2*e* shows the strongest initial rise, as the concave upward surface relief initially matches the pulse shape reasonably closely.

Computations of the types shown in figure 2 are necessary to improve design specifications for the operation of satellite altimeters over ice sheets. Although little three-dimensional mapping of the ice sheet surface of the higher parts of Greenland and Antarctica is available, the considerable amount of linear profiling from aircraft and surface vehicles now available should be sufficient to draw up adequate specifications. Laser profiling with an accurately positioned footprint of 100 m or less would overcome many difficulties due to the broad footprint of a radar altimeter over an undulating ice surface.

(*e*) *Sea ice*

Figure 1*d* shows four consecutive pulse shapes 6.6 km apart as the satellite moves out over the edge of the pack ice. The third pulse shows a strong early peak typical of the glistening shown by pack ice returns. The fourth pulse appears similar to the open ocean pulse shapes of figure 1*a*. Although pulses in figure 1*d*(i) and (ii) do not show the glistening, they show a rapid pulse rise compared with the fourth pulse, indicating that the wave height is much lower for the two pulses inside the outer band of pack ice. Figure 1*e* shows a series of four consecutive pulses well within the pack ice near the coast. The first three pulses show particularly strong 'glistening' returns typical of pack ice while the fourth shows very little glistening. The vertical scale of figure 1*e*(ii) and (iii) is 600 units, figure 1*e*(i) covers 450 units and figure 1*e*(iv) only 100 units. Apart from the enhanced glistening effect on figure 1*e*(i)–(iii) the remainder of the pulses are all of similar form and amplitude to figure 1*e*(iv).

From inspection of all 94 pulse shapes recorded from the coast to the open ocean, only 8 showed no clear glistening characteristic. These included five of the outermost ten records, where one may expect belts of pack ice alternating with stretches of open water. Variations of glistening with location and with season appear likely and require 'surface truth' observations. However, it appears reasonable to attribute the glistening effect to the absence of ripples or wavelets that give ocean surface pulses a diffuse character. Such ripples are damped out completely by any thin film of ice, leaving long wavelengths to govern surface slopes that produce glistening returns. Few direct slope measurements within pack ice are available, but figure 3 shows slopes calculated from wave-energy spectra measured by Squire & Moore (1980) by using vertical accelerometers on ice floes in the Bering Sea for periods above 4 s (25 m wavelength). Even at this wavelength, the outer floes of 10 m diameter damp out most wave energy within 5 km, as shown also in figure 1*d*.

Sea surface slopes result from the combined effect of all frequency bands of figure 3 and can

PHILOSOPHICAL TRANSACTIONS OF THE ROYAL SOCIETY A MATHEMATICAL, PHYSICAL & ENGINEERING SCIENCES

be estimated from the period of maximum energy and significant wave heights derived from figure 3. Resultant slopes range from 1.6×10^{-2} at the ice edge, 1.2×10^{-2} at 5 km to 2.7×10^{-3} at 65 km from the edge. The last slope is close to the value of 3×10^{-3} derived from the width of the pulse in figure 1*d* (iii) and equation (12), which should be typical of regions with broken floes in moderate weather.

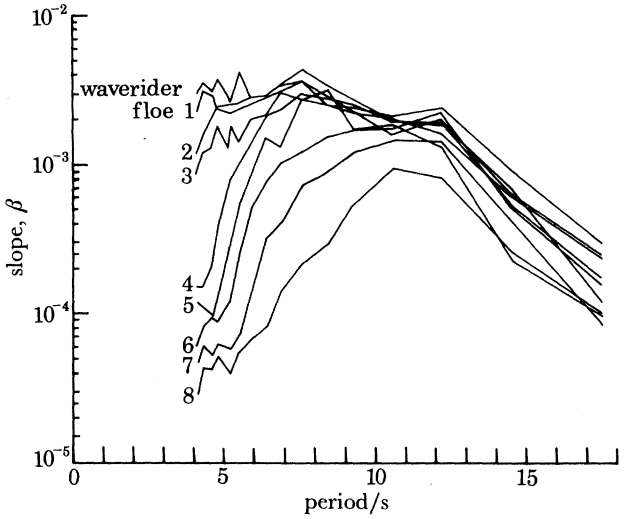

FIGURE 3. Surface slopes of the marginal ice zone of the Bering Sea derived from measured wave-energy spectra in frequency bands given in Squire & Moore (1980). The waverider buoy record was obtained just outside the ice edge, that from floe no. 1 at the ice edge, no. 2 at 0.7 km, no. 3 at 2.2 km, no. 4 at 5.3 km, no. 5 at 10.3 km, no. 6 at 18.9 km, no. 7 at 38.6 km and no. 8 at 65.1 km from the ice edge. Ice floes were typically 10 m in diameter from 0 to 5 km, then increased gradually to 40 m at 30 km, after which the floe size increased abruptly to greater than 100 m.

Not all pack ice consists of thin newly frozen ice; older ice typically has a rough surface, new ice is usually covered after a few days by snow, and open water between floes will be rippled by any wind of appreciable strength. Because these surfaces may produce a diffuse echo the reason for the dominant glistening echo from sea ice needs further explanation. This comes from considering the relative strengths of the two types of return. If equal areas contribute to the power of glistening (P_{rg}) and diffuse (P_{rd}) returns, we can calculate the ratio of energies involved by dividing (11) by (10), and putting $S_r = g_t \lambda^2 / 4\pi$. This gives

$$P_{rg}/P_{rd} = \frac{R_g}{R_d} \frac{r_0^{\frac{1}{2}}}{4(vt)^{\frac{1}{2}}} \frac{1}{\beta_{max}}. \tag{14}$$

For a satellite height of 800 km, $\beta_{max} = 3 \times 10^{-3}$ and other parameters for Seasat and ERS-1 in table 2, we get $P_{rg}/P_{rd} = 8.5 \times 10^4 R_g/R_d$. Because the power reflexion coefficient for thin sea ice is typically 7 dB higher than for a snow/firn surface, for equal areas of glistening and reflexion $P_{rg}/P_{rd} \approx 5 \times 10^5$.

The glistening character of the pulse shape will still be quite obvious for a ratio P_{rg}/P_{rd} of 50 when less than 0.01 % of the surface is producing the glistening type of echo. Thus, provided that a small area of new ice or calm water is exposed, as is likely at the locations and season of pulses shown in figure 1*d*, *e*, the dominant glistening characteristic is explicable.

When surface slopes due to wave action are small well inside the pack ice zone, we expect intermittent returns of a specular nature from new sea ice and open water leads (when calm).

PHILOSOPHICAL TRANSACTIONS OF THE ROYAL SOCIETY A MATHEMATICAL, PHYSICAL & ENGINEERING SCIENCES

Strong specular returns, when averaged over 100 pulses, should still dominate the pulse shape if any significant specular reflexion is present as in the first three pulses of figure 1*e*. However, with large floes many kilometres across, the glistening effect will be intermittent if the remainder of the surface follows Lambert's law, as shown in the fourth pulse of figure 1*e*. The presence of large ponds on the surface of Arctic pack ice in summer, when newly frozen or in calm weather, may also produce glistening. Indeed, our calculation suggests that glistening could be much stronger still than that shown in figure 1*d*, *e*. Furthermore, a search for glistening-type returns from very calm seas and lakes in lower latitudes may provide a rapid means of identifying regions where wind speeds are too low to produce surface ripples.

The varying surface of an ice-covered ocean described earlier will clearly give wide variations in reflected energy, often within the area covered by one pulse. The evaluation of such surfaces from satellite-derived data will clearly benefit from an analysis of many different parameters, such as passive microwave radiation, scatterometry, synthetic aperture radar and altimeter pulse shapes, all of which can operate through clouds and in darkness and supplement the higher-resolution imagery at optical and infrared wavelengths.

The authors acknowledge valuable help from Dr H. J. Zwally of N.A.S.A.–Goddard Spaceflight Center, who made available tapes of Seasat data, and assistance with aspects of this study by N. McIntyre, M. R. Gorman and A. P. R. Cooper of the S.P.R.I.

REFERENCES

Booker, H. G., Ratcliffe, J. A. & Shinn, D. H. 1950 *Phil. Trans. R. Soc. Lond.* A **242**, 579–607.
Brooks, R. L. 1982 *Ann. Glaciol.* **3**, 32–35.
Brooks, R. L., Campbell, W. J., Ramsier, R. O., Stanley, H. R. & Zwally, H. J. 1978 *Nature, Lond.* **274**, 539–543.
Budd, W. F. 1970 *J. Glaciol.* **9**, 19–27.
Budd, W. F. & Jenssen, D. 1975 *Int. Ass. Sci. Hydrol. Publ.* no. **104**, pp. 257–291.
Budd, W. F., Jenssen, D. & Radok, U. 1971 *Nature, phys. Sci.* **232**, 84–85.
Budd, W. F. & Smith, I. N. 1981 *Int. Ass. Sci. Hydrol. Publ.* no. **131**, pp. 369–409.
Beckmann, P. & Spizzichino, A. 1963 *The scattering of electromagnetic waves from a rough surface*. London: Pergamon Press.
Collins, I. F. 1968 *J. Glaciol.* **7**, 199–204.
Cooper, A. P. R., McIntyre, N. F. & Robin, G. de Q. 1982 *Ann. Glaciol.* **3**, 59–64.
Crary, A. P. 1962 *IGY Glaciol. Rep.* no. 6. New York: American Geographical Society.
Drewry, D. J. 1981 In *Remote sensing in meteorology, oceanography and hydrology* (ed. A. P. Cracknell), pp. 270–284. Chichester: Ellis Horwood.
Drewry, D. J., Jordan, S. R. & Jankowski, E. J. 1982 *Ann. Glaciol.* **3**, 83–91.
Glen, J. W. 1955 *Proc. R. Soc. Lond.* A **228**, 519–538.
Goodman, D. J., Wadhams, P. & Squire, V. A. 1980 *Ann. Glaciol.* **1**, 23–27.
Jacobs, S. S., Gordon, A. L. & Ardai, J. L. Jr 1979 *Science, Wash.* **203**, 439–443.
Mae, S. & Naruse, R. 1978 *Nature, Lond.* **273**, 291–292.
Martin, S. 1981 *A. Rev. Fluid Mech.* **13**, 379–397.
Neal, C. S. 1979 *J. Glaciol.* **24**, 295–307.
Nye, J. F. 1951 *Proc. R. Soc. Lond.* A **207**, 554–572.
Paterson, W. S. B. 1981 *Physics of glaciers*, 2nd edn. Oxford: Pergamon.
Radok, U. 1978 *Climatic roles of the ice*. Paris: Unesco.
Robin, G. de Q. 1963 *Phil. Trans. R. Soc. Lond.* A **255**, 313–339.
Robin, G. de Q. 1966 *Can. J. Earth Sci.* **3**, 893–901.
Robin, G. de Q. 1967 *Nature, Lond.* **215**, 1029–1032.
Robin, G. de Q. 1968 In *Symposium on Antarctic oceanography* (ed. R. I. Currie), pp. 191–197. Cambridge: Scott Polar Research Institute for SCAR.
Robin, G. de Q. 1983 *The climatic record in polar ice sheets*. Cambridge University Press.
Robin, G. de Q., Evans, S. & Bailey, J. T. 1969 *Phil. Trans. R. Soc. Lond.* A **265**, 437–505.
Sergin, V. Ya. 1979 *J. geophys. Res.* **84** (C6), 3191–3204.

PHILOSOPHICAL TRANSACTIONS OF THE ROYAL SOCIETY A MATHEMATICAL, PHYSICAL & ENGINEERING SCIENCES

Squire, V. A. & Moore, S. C. 1980 *Nature, Lond.* **283**, 365–368.
Swithinbank, C. W. M. 1962 *Norsk Polarinst. Årb.* **196**, 28–31.
Swithinbank, C. W. M., McLain, P. & Little, P. 1977 *Polar Rec.* **18**, 495–501.
Tchernia, P. 1974 *C.r. hebd. Séanc. Acad. Sci., Paris* D **278**, 667–670.
Thomas, R. H. 1973 *Br. antarct. Surv. sci. Rep.* no. 79.
Thomas, R. H. 1979 *J. Glaciol.* **24**, 167–177.
Vialov, S. S. 1958 *Int. Ass. Sci. Hydrol. Publ.* no. 47, pp. 266–275.
Wadhams, P. 1975 *J. Geophys. Res.* **80**, 4520–4528.
Wadhams, P. 1978 *Deep Sea Res.* **25**, 23–40.
Weertman, J. 1957 *J. Glaciol.* **3**, 33–38.
Zotikov, I. A., Zagorodnov, V. S. & Raiskovsky, J. V. 1980 *Science, Wash.* **207**, 1463–1465.
Zwally, H. J. 1975 *J. Glaciol.* **15**, 444.
Zwally, H. J. & Gloersen, P. 1977 *Polar Rec.* **18**, 431–450.

Discussion

A. S. Laughton, F.R.S. (*Institute of Oceanographic Sciences, Wormley, Godalming, U.K.*). Dr Robin reported the inability of the altimeter on ERS-1 to cope with the rough topography of the margins of the polar regions, and in particular its inability to record the bottoms of steep-sided valleys. The geometrical problems of altimetry are essentially similar to those of standard echo-sounders in the ocean, which have been studied for decades by marine geophysicists. The rise time of the first return and the subsequent reverberation time are both measures of surface roughness, the surface in echo-sounding being the sea floor. Larger-scale sea-floor topography is represented by the superposition of hyperbolae arising from the multiplicity of point reflectors, which give a record that can be analysed, by migration techniques now highly developed in the oil prospecting industry.

The major difference between altimetry and echo-sounding is that whereas the former uses gating techniques to lock onto first arrival echoes and rejects any subsequent data, the latter records all returns. Could the coarse topography over the marginal polar regions be better measured by widening the receive gates on the altimeter and relaying back to Earth the multiple pulses, which could then be analysed to give the required information?

G. de Q. Robin. In principle the answer is yes. At the Scott Polar Research Institute we have developed these migration techniques for improving our analysis of bedrock topography obtained by radio echo-sounding of the ice sheet. With radar altimetry from satellites the problem is one of data acquisition and handling. If the time gate for data acquisition is lengthened we have to decrease the accuracy of elevation measurement because of constraints on data transmission for ERS-1 as currently planned. The alternative of greatly increasing the amount of data transmitted would add very considerably to the costs. This may only be justified if extra information obtained on the surface form of the ice sheet is of critical importance to scientific knowledge.

PHILOSOPHICAL TRANSACTIONS OF THE ROYAL SOCIETY A MATHEMATICAL, PHYSICAL & ENGINEERING SCIENCES